THE BELL SYSTEM
TECHNICAL JOURNAL

VOLUME XLIII MAY 1964 NUMBER 3

Digital Light Deflection

By T. J. NELSON

(Manuscript received July 30, 1963)

A digital method of deflecting a light beam using n optical modulators and n uniaxial crystals to provide 2^n positions of the beam is described. The input-output relations for one special configuration are derived. Optical problems and limitations are investigated and, in particular, it is found that the upper limit to the density of positions is about 10^6/sq. in. Presently available modulators are considered, and it is found that a KDP modulator has a power limitation above 1 mc operation for a total number of positions of about 70,000. Finally, the applications of the method as a semipermanent memory, a PCM decoder, and a digital delay line are briefly considered.

I. INTRODUCTION

It is desirable to substitute a light beam for the electron beam used in the class of devices of which the flying spot scanner and the Williams tube are examples. In this class of devices the electron beam is used to probe a suitable target and read or store information on it. The substitution is desirable because a light beam has negligible inertia and can, in principle, be deflected rapidly. The subject of this paper*, †, ‡ is a new

* The contents of this paper were discussed by the author at the Twenty-First Annual Conference on Electron Device Research (IEEE), Salt Lake City, Utah, June 26–28, 1963.

† A brief description of methods that can be used to deflect a light beam is given by U. J. Schmidt (Schmidt, U. J., The Problem of Light Beam Deflection at High Frequencies, Proceedings of the Symposium on Optical Processing of Information, ed. Pollack, D. K., Koester, C. J., and Tippett, J. T., Spartan Books, Inc., Baltimore, 1963, p. 98).

‡ *Note Added in Proof*. An article on some aspects of digital light deflection has recently appeared in the literature: see Kulcke, W., Harris, T. J., Kosanke, K., and Max, E., IBM Journal of Research and Development, **8**, 1964, pp. 64–67.

method of deflecting a light beam. This method, which is called digital light deflection, employs n optical modulators and n uniaxial crystals. By applying appropriate two-level electrical inputs to the n optical modulators, it is possible to deflect a light beam to 2^n positions. This deflection technique is inherently digital and the required optical modulator inputs are binary signals.

In the present paper we shall consider:

(a) the basic principles of digital light deflection

(b) the address logic for a special configuration

(c) optical problems which limit the density of positions that can be achieved

(d) presently available optical modulators and the speed limitations which they impose on a digital light deflection system

(e) experimental results that have been obtained with a four-unit (16-position) digital light deflection system.

II. PRINCIPLES OF DIGITAL LIGHT DEFLECTION

2.1 *The Binary Unit*

It is well known that uniaxial crystals have the property of displacing light of one polarization, called the extraordinary ray, while the orthogonal polarization, the ordinary ray, obeys Snell's law. If the two rays are parallel upon entering the crystal, they will be parallel upon leaving, but are not parallel inside the anisotropic medium.

Fig. 1 shows a uniaxial crystal oriented so that its optic axis lies in an xz plane. If the electric field vector of a plane-polarized beam is in the

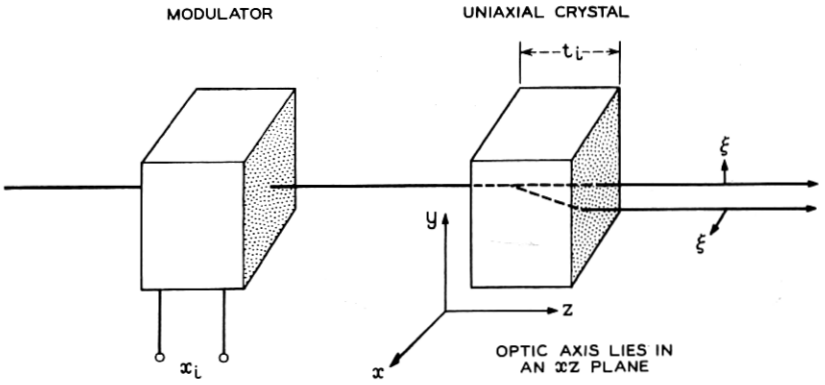

Fig. 1 — The binary unit.

x direction, it will be displaced by an amount proportional to the thickness of the crystal. The exact dependence of the deflection on the crystal thickness and orientation is given in Appendix A. If the beam is polarized in the y direction, its electric field vector is normal to the optic axis, and the beam will pass through the crystal in a straight line.

If a modulator precedes the uniaxial crystal and is capable of rotating the plane of polarization from the x direction to the y direction, and inversely, under the influence of an input signal, then it is possible to switch the beam from one position to another. Furthermore, an error in the input signal will cause the beam to be split and light transmitted simultaneously to the two positions, rather than to some other position, as would be the case with an analog deflector.

The combination of optical modulator and uniaxial crystal, in Fig. 1, is referred to as a binary unit. Because the use of a multiplicity of binary units will be considered next, subscripts identify the variables of a particular binary unit. For example, t_i represents the thickness of the uniaxial crystal in the ith binary unit and x_i describes the state of the ith modulator. If $x_i = 1$, then the plane of polarization of the incident light beam is rotated 90° by the ith modulator; whereas if $x_i = 0$ the rotation is zero.

2.2 *The Deflection Bank*

If a linearly polarized light beam is made to traverse a sequence of n binary units of the type described, then a maximum of 2^n positions of the beam can be realized. Such a combination of n binary units is designated as a deflection bank, and if the deflections are all in the x direction, as the x-deflection bank. The resulting pattern of deflections produced by a bank depends upon the thickness and orientation of the various uniaxial crystals in the bank.

A linear pattern of 2^n positions, uniformly separated, can be obtained with an n-unit bank if all uniaxial crystals have the same orientation and if their thicknesses are respectively $t_0, 2t_0, \cdots, 2^{n-1}t_0$. If the beam displacement in the thinnest crystal is d_0, then the separation between positions is also d_0. Each binary unit in such a bank is unique, as its uniaxial crystal differs in thickness from all other uniaxial crystals. The binary units in such a linear deflection bank may be arranged in any order, but we shall confine any further discussion to a configuration where the light beam successively encounters uniaxial crystals of thickness given by

$$t_i = 2^{n-i}t_0; \qquad i = 1, 2, \cdots, n. \tag{1}$$

This configuration will be shown later to have interesting and desirable properties.

A three-unit example of the configuration that has been singled out is shown in Fig. 2. The polarization of the beam before it enters the bank is orthogonal to the optic axes of the uniaxial crystals and the thickness of successive uniaxial crystals decreases by two. The two columns at the right of Fig. 2 give the positions of the beam in binary form and the modulator inputs which are required to deflect the beam to these positions.

2.3 *Address Logic*

In this section, a derivation of input-output relations and a discussion of code conversion are given for the special linear bank configuration which was mentioned in the previous section.

2.3.1 *Input-Output Relations*

For the purpose of deriving the deflection as a function of the modulator inputs, it is assumed that the polarization of the beam, as it enters the bank, is orthogonal to the optic axes of the uniaxial crystals in the bank. Then if none of the modulators are operated, the beam is undeflected by the bank. Since the displacement of the beam by unit i is determined by the plane of polarization of the beam after it has passed the modulator in unit i, whether deflection occurs is determined by the number of times the polarization of the beam has been rotated up to, and

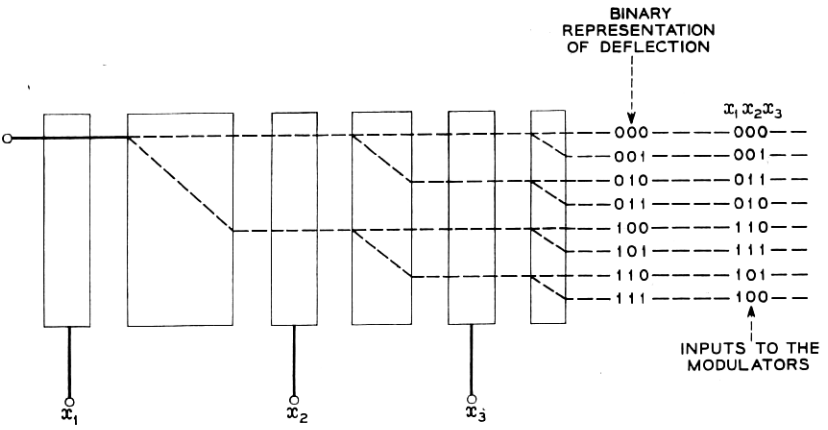

Fig. 2 — Three-unit deflection bank.

including, unit i. If we designate the deflection at unit i as a binary variable, d_i, then the displacement of the beam is $2^{n-i} d_0$ if $d_i = 1$ and 0 if $d_i = 0$. The general formula for the deflection is

$$d_i = S_{\text{odd}}(x_1, x_2, \cdots, x_i) \tag{2}$$

and

$$d_x = \sum_{i=1}^{n} 2^{n-i} d_i d_0 \tag{3}$$

where d_x is the total deflection of the beam in the x-deflection bank. S_{odd} is the notation for a symmetric switching function and its value is one if an odd number of the indicated variables have the value one, and zero otherwise.[1] Thus unit i will add its displacement to the total if the polarization of the beam has been rotated an odd number of times up to, and including, the ith unit.

The use of (2) and (3) is illustrated by considering the three-unit bank in Fig. 2. Suppose the input to the modulators is

$$x_1 x_2 x_3 = 111$$

and we wish to find the corresponding deflection. According to (2) we count, starting from the left, the number of ones appearing up to and including the position under consideration. If the result is odd we enter a one at the corresponding position of the deflection variable. Hence in this case

$$d_1 d_2 d_3 = 101.$$

Substitution of these deflection variables into (3) yields that the total deflection $d_x = 5d_0$.

In general, the addressing or input-output relations have not been completely specified until the inverses of (2) and (3) are given. If we desire to have unit i add its contribution to the total displacement but not unit $i - 1$, or if we desire the displacement of unit $i - 1$ but not that of unit i, then it is clear that the modulator in unit i must rotate the plane of polarization of the beam. This fact is the inverse of (2) and is expressed by

$$x_i = S_{\text{odd}}(d_{i-1}, d_i). \tag{4}$$

The inverse of (3) merely translates the binary number $x_1, x_2, \cdots, x_n$ from base two to base ten.

$$X = \sum_{i=1}^{n} 2^{n-i} x_i. \tag{5}$$

The use of (4) is apparent if we again consider the three-unit bank in Fig. 2. Suppose a total deflection $d_x = 5d_0$ is desired and we wish to find the necessary inputs; then (4) is appropriate. First, however, (3) is used to obtain the deflection variables d_i. Use of (3) gives in this example, as we have seen before, $d_1d_2d_3 = 101$. According to (4), if an entry in the deflection variable differs from the preceding entry, the corresponding entry in the modulator variable x_i is a one. Since the last two entries in $d_1d_2d_3 = 101$ are 01, then $x_3 = 1$. Proceeding in this fashion we obtain

$$x_1x_2x_3 = 111$$

which is the expected result.

An interesting and desirable property of the configuration that has been considered is that it is always possible to switch the beam to adjacent positions by changing the state of excitation of just one modulator. This is apparent for the three-unit bank in Fig. 2. To show this in general, consider the highest numbered unit, j, for which the number of rotations of the plane of polarization up to and including unit j is even. Evidently, all the units following j add their contributions to the total displacement. Since

$$2^j - 1 = 2^{j-1} + 2^{j-2} + \cdots + 2^{j-j+1} + 2^0 \qquad (6)$$

we have only to change the state of excitation to modulator j to increase the total deflection by the incremental distance, d_0. Also, consider the highest numbered unit, k, for which the number of rotations up to and including unit k is odd. Then unit k adds its contribution to the total deflection, but none of the units following k do. Hence, by changing the state of excitation to the modulator in unit k, we decrease the deflection by d_0. The reasoning breaks down in the first case if the excitation is $100 \cdots 0$, where the number of rotations is odd for all units, and in the second case if the excitation is $00 \cdots 0$. However, the total deflection is then either a maximum or zero, and these two conditions are reached from each other by changing the state of excitation to the modulator in unit 1. Hence the input-output relations for this configuration are cyclic; i.e., adjacent positions can always be reached from each other by changing the state of excitation to exactly one modulator.

2.3.2 *Code Conversion*

One can ask, what type of operation can be performed on the input signals to further simplify the input-output relations? If the inputs to a switching network are designated by the W_i's and the outputs by the x_i's, which are, as before, the direct inputs to the modulators, one type of

code conversion could be

$$x_i = S_{\text{odd}}(W_{i-1}, W_i). \tag{7}$$

It is known from (4) that

$$x_i = S_{\text{odd}}(d_{i-1}, d_i); \tag{8}$$

hence, from an inspection of (7) and (8) it is evident that

$$d_i = W_i.$$

Thus, the deflection and input variables are caused to be the same binary numbers. If the W_i's are the outputs of a series of bistable multivibrators which are triggered from a series of harmonically related sine waves, then $W_1, W_2, \cdots, W_n$ and hence $d_1, d_2, \cdots, d_n$ assume the binary numbers in increasing order, and a linear sweep would thereby be effected.

Fig. 3 shows the details of one switching network which can be used for

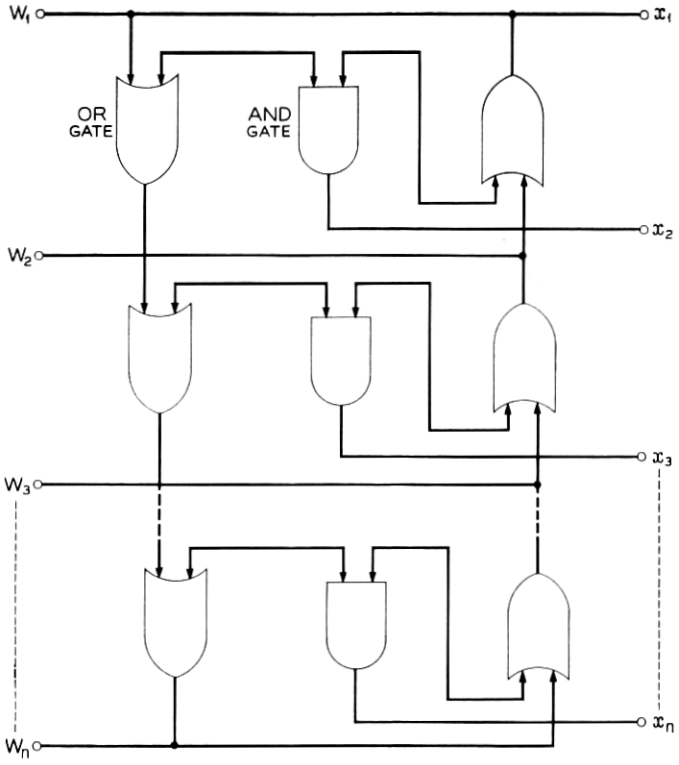

Fig. 3 — Code conversion network.

such code conversion. Two AND gates and one OR gate per binary unit are required, with the exception of the input to unit 1, which requires no alteration.

III. OPTICAL CONSIDERATIONS OF DIGITAL LIGHT DEFLECTION

3.1 *Incorporation of Lens System*

Up to this point, consideration has been limited to plane waves; however, a higher density of resolvable positions is achieved with focused light. If an x-deflection bank and a y-deflection bank are incorporated into the object and image spaces of a lens as shown in Fig. 4, it is possible to focus an aperture into the image plane in a rectangular array of positions. The extra modulator which precedes the y-deflection bank in Fig. 4 insures that the input polarization to the y bank is in the x direction. To accomplish this, the input to the modulator, T, must then be given by

$$T = S_{\text{even}}(x_1, x_2, \cdots, x_n)$$

where S_{even} is a symmetric function whose value is one if an even number of the indicated x variables have the value one, and zero otherwise. Thus, the deflection in the y direction, dx, is related to the y variables in the same manner as the deflection in the x direction, dx, is related to the x variables. Hence the input-output relations developed in the previous section apply to both the x bank and the y bank.

If there are n units in the x bank and m units in the y bank, then the resulting pattern is a matrix of $2^n \times 2^m$ positions. The incorporation of a

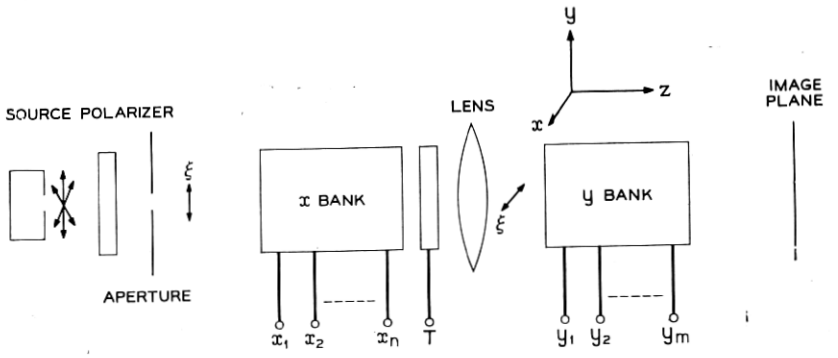

Fig. 4 — Incorporation of x bank and y bank into lens system.

lens into the system causes the rays through the system to have a range of angles with the z axis. Since the deflection in the uniaxial medium is angle-dependent, the maximum angle must be kept small. The optical modulators also limit the range of angles that are tolerable.

For simplicity in the following discussions, the distance from the aperture to the lens is assumed equal to the distance from the lens to the image plane. That is to say, the optical system has unity magnification. This simplifies some of our considerations with little loss in generality, and also unity magnification probably would be used in any practical system.

3.2 *Diffraction Effects*

Because of the anisotropy of the uniaxial crystals and possibly the modulator crystals, we require a high f number for the system. However the minimum resolvable separation between spots is roughly proportional to the f number. If the ratio of the focal length of the lens to the diameter of the lens opening is 15, that is, $f/15$, then the maximum angle any ray through the system can have with the axis of symmetry is $3/\pi$ degrees. The following calculations are based on this compromise.

We define the crosstalk ratio to be

$$C = 10 \log_{10} [P(0)/P(d)] \tag{9}$$

where $P(0)$ is the integrated intensity falling on a circle of radius a, the radius of the aperture, centered on the image and $P(d)$ is the integrated intensity falling in a circle of radius a separated from the image by a center-to-center distance of d. Fig. 5 shows curves of constant cross-

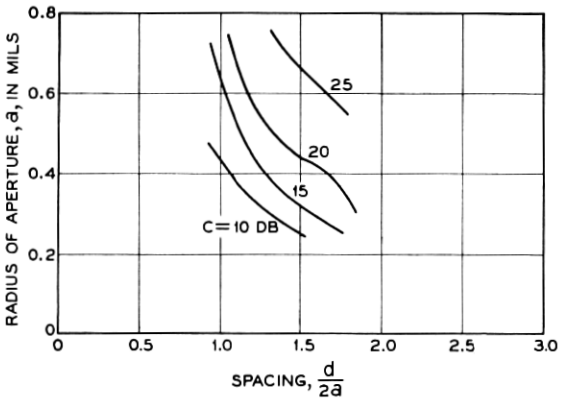

Fig. 5 — Radius of aperture vs center-to-center spacing at constant crosstalk, $f/15$ and 6943 Å.

talk ratio plotted with a as ordinate and $d/2a$ as abscissa. Fig. 6 is a plot of the loss from the integrated intensity admitted by the aperture to that falling on a circle of radius a centered on the image. These data were obtained by numerically evaluating the integrals derived in Appendix B. Figs. 5 and 6 are given for $f/15$ and $\lambda = 6943$ Å. Plane wave illumination of the aperture was assumed, and small angle approximations were made.

From the standpoint of crosstalk, no optimum seems to exist, although we find that for $a = 0.3$ mil and $d = 1.1$ mils, the value $C = 20$ db results. Therefore we find that the spot density, D, can be made as high as

$$D = \frac{1}{(1.1 \times 10^{-3})^2} = 0.826 \times 10^6/\text{in}^2$$

at $f/15$, and 6943 Å. Fig. 6 indicates that the loss would be 11 db for this case.

3.3 *Refractive Index Effects*

In general, a deflected beam passes through some of the uniaxial crystals as an extraordinary beam; hence it encounters a different refractive index from the undeflected beam which passes through all crystals as an ordinary beam. As a result the deflected image of the aperture will be formed at a different z coordinate in the optical system than the undeflected image. For paraxial imaging, which is consistent with our assumption of a fairly large f number, a calculation yields that this shift in the image is given by

$$\Delta Z = (Z_d - Z_0) = \left(\frac{n}{n_r^2} - \frac{1}{n_0}\right) \cot \psi [dx + dy] \qquad (11)$$

where Z_d is the z coordinate of the deflected image and Z_0 is the z co-

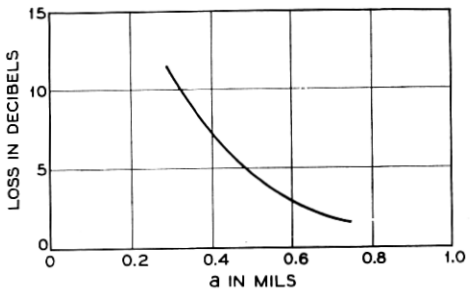

Fig. 6 — Loss vs radius of aperture at $f/15$ and 6943 Å.

ordinate of the undeflected image. Here z is positive in the image space and is measured from the center of the lens. Also, dx and dy are the x and y displacements of the deflected image. In (11)

$$n = \left(\frac{n_0^2 + n_e^2}{2}\right)^{\frac{1}{2}}, \tag{12}$$

$$n_r^2 = 2n_0^2 n_e^2/(n_0^2 + n_e^2) \tag{13}$$

and for the orientation ψ of the uniaxial crystal which gives the largest deflection (see Appendix A)

$$\cot \psi = 2n_e n_0/(n_0^2 - n_e^2). \tag{14}$$

The refractive indices of calcite at 589 mμ are[2]

$$n_0 = 1.65803, \qquad n_e = 1.4864 \tag{15}$$

hence from (11), (12), (13), (14) and (15)

$$\Delta Z = 0.36\, dx + 0.36\, dy. \tag{16}$$

We should note that since this is indeed the equation of a plane, we have merely to tilt any target to be used at the appropriate angle to get a sharp image at each of the possible positions of the spot.

IV. OPTICAL MODULATORS

Two possible ways of achieving 90° rotation of the plane of polarization have been investigated. A high specific rotation is possible in yttrium iron garnet in a magnetic field due to the Faraday effect. The necessary fields are quite high, however, for 90° rotation in a crystal of reasonable thickness; moreover, YIG has high optical attenuation at the wavelengths for which the specific rotation is greatest.[3]

Due to the linear Pockels effect, a ZO plate of KH_2PO_4 can cause 90° rotation with the half-wave voltage applied in the z direction if the induced principal axes are at 45° to the x and y directions.[4] Since KDP is a ferroelectric, the half-wave voltage is directly proportional to the temperature above the Curie temperature.

Fig. 7 defines the dimensions and orientation of a KDP crystal to be considered for a modulator.

The clamped dielectric constant, loss tangent, and half-wave voltage in the z direction are,[5,6]

$$\epsilon \approx \frac{2.27 \times 10^3 + 4.7T}{T - 119} \tag{17}$$

$$\tan \delta \approx \frac{8.42 \times 10^{-1}}{T - 119} \tag{18}$$

$$V_{\lambda/2} \approx 42(T - 119) \text{ volts.} \tag{19}$$

The stored energy and the dissipated energy per cycle are

$$W_S = \tfrac{1}{2} C V_{\lambda/2}^2 \tag{20}$$

$$\approx \{1.77 + 3.67 \times 10^{-3} T\} (T - 119) \times 10^{-7} (ab/c) \text{ joules} \tag{21}$$

$$W_{\text{dis}} = 2\pi W_S \tan \delta \tag{22}$$

$$\approx \{0.938 + 1.94 \times 10^{-3} T\} \times 10^{-6} (ab/c) \text{ joules} \tag{23}$$

where the dimensions a, b, and c are the dimensions of the crystal in the x, y, and z directions, respectively, and are understood to be in centimeters.

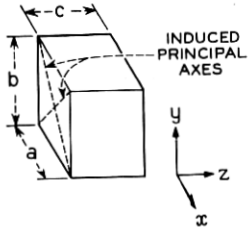

Fig. 7 — Dimensions of KH_2PO_4 modulator.

In the section on diffraction, we noticed that the center-to-center spacing of the spots would have to be greater than about one mil. If there are eight binary units in the x-deflection bank and eight in the y bank, then a square array of 65,536 positions results, 256 on a side. If the incremental spacing is one mil, then with some loss in intensity to the spots on the edge of the pattern we could choose the diameter of the lens opening, and hence a and b, to be 1 cm.

For this relatively small number of positions, and for a KDP modulator as thick as 1 cm, the dissipated energy per cycle will be on the order of one microjoule. To reduce the stored energy per cycle to this value, we would have to cool the modulator to about 6° above its Curie temperature. Thus a KDP modulator has a severe power limitation for nominal system capacities, if operation above 1 mc is desired.

V. EXPERIMENTAL RESULTS

In order to examine the optical limitations of digital light deflection, a four-unit system has been constructed. Fig. 8 is a pictorial diagram and

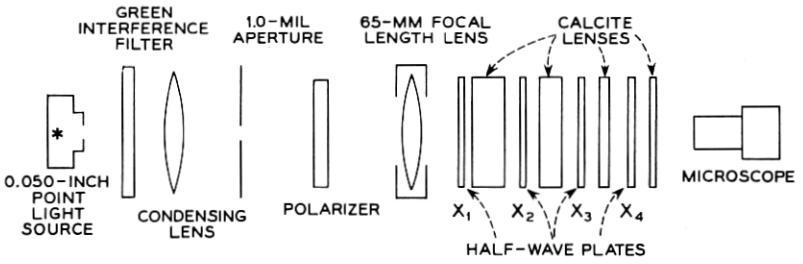

Fig. 8 — Pictorial diagram of four-unit deflection system.

Fig. 9 is a photograph of the experiment. The essential elements are: a 50-mil point light source which illuminates a 1.0-mil diameter aperture, a 65-mm lens which focuses the aperture at unity magnification into the image plane, a four-unit deflection bank, and a microscope for viewing the real image of the spot in the image plane. The four-unit deflection bank consists of four rotators and four calcite disks. The rotators were constructed by aligning two disks of Bausch and Lomb quarter-wave plastic. The rotators were mounted so that they could be rotated through 45°. In one orientation the principal directions of the so-constructed half-wave plate were parallel to the two possible polarizations of the beam and there was no rotation. In the other orientation the principal direc-

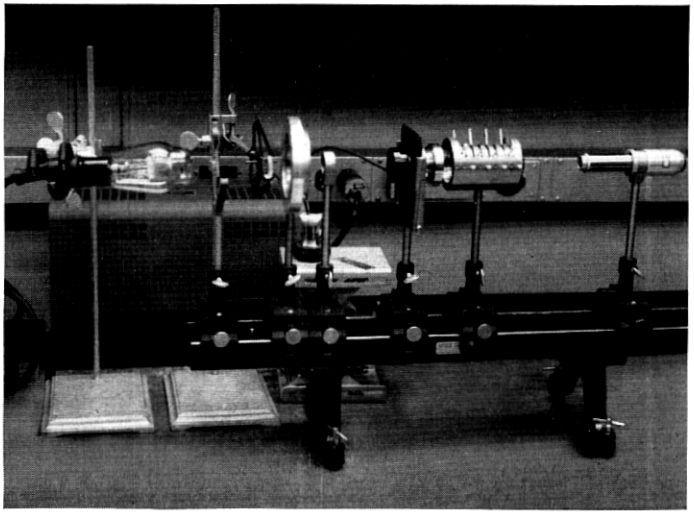

Fig. 9 — Photograph of four-unit experiment.

tions of the half-wave plate were at 45° to the possible polarizations of the beam, and the polarization of the beam was rotated by 90°.

The system was designed to give 16 positions of the 1.0-mil spot, with center-to-center distances of 2.5 mils. This design called for calcite disks of 0.0266, 0.0452, 0.0903, and 0.1806 in. thick. The disks obtained were 0.020, 0.045, 0.090, and 0.180 in. thick, the largest error occurring in the thinnest disk.

It was found that, for the maximum deflection of nominally 37.5 mils, the dispersion of the calcite in the deflection was about 1.0 mil over the visible spectrum. The half-wave plates were found to pass appreciable amounts of the unwanted polarization at the red end of the spectrum, and the dichroic polarizer used was known to be less efficient at the blue. For these reasons, the cleanest spot pattern was obtained with a green filter. It was further found that the relative intensity of the diffraction rings increased appreciably above an f number of 22. Figs. 10 and 11 are photographs of the spot pattern for various modulator settings with white and green light, respectively. The nomenclature $x_1x_2x_3x_4$ has the same meaning as that described above. These photographs were taken through the microscope at $f/22$ and $f/16$ of the lens and camera respectively, and the exposure times are indicated. The photographs show that the error in the thinnest calcite disk causes a noticeable "pairing" of the spots.

In order to provide a check on the diffraction analysis, we set the lens opening to $f/15$ and used a 666-mμ filter. The spot pattern was enlarged six times, and a 6-mil diameter aperture was centered at the position of the first spot in the new image plane. The light transmitted through this aperture was then detected by a photomultiplier. With this arrangement, x_4 was alternated, and the resulting change in photomultiplier current noted. These first two spots are "paired," as may be easily seen by inspecting Figs. 10 and 11. We measured their center-to-center spacing in the red light to be 1.04 ± 0.25 mils. For $f/15$, $\lambda = 694\ \mu$, and $d = 1.04$ mils, the predicted value of the crosstalk ratio is 12.8 db, whereas the measured value was 10.2 db.

VI. APPLICATIONS

There are many functions that could be performed by digital light deflection. We shall briefly discuss three: a semipermanent memory, a pulse code modulation (PCM) decoder, and a digital delay line. In these applications, deflection banks similar to those described above can be used. The principal differences reside in the numbers of possible positions of the beam and the type of target used.

X_1, X_2, X_3, X_4 IN
INTERMEDIATE SETTINGS
20 SECONDS

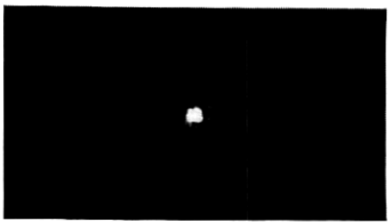

$X_1, X_2, X_3, X_4 = 0000$
5 SECONDS

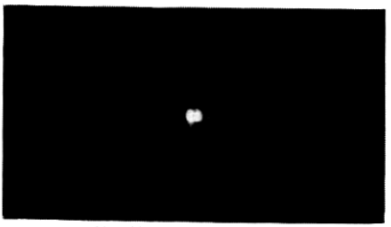

$X_1, X_2, X_3, X_4 = 1010$
5 SECONDS

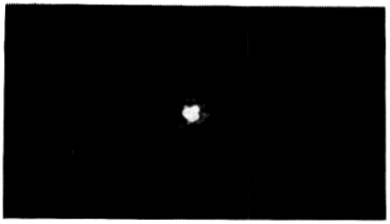

$X_1, X_2, X_3, X_4 = 0101$
5 SECONDS

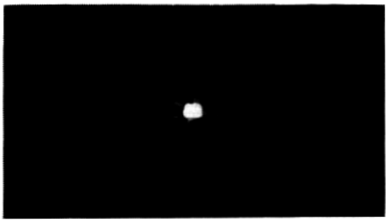

$X_1, X_2, X_3, X_4 = 1000$
5 SECONDS

Fig. 10 — Microphotographs of spot patterns with no filter.

6.1 *The Semipermanent Memory*

Digital light deflection may be used to provide access to a target where information is stored in the form of a matrix of potential light paths. We place a photomultiplier tube, or some other photosensitive device, behind the target. When one of the possible combinations of inputs is applied to the modulators, the beam falls on the position of the target corresponding to that combination. If the target is transparent at that position, then we get an output from the photosensitive device which

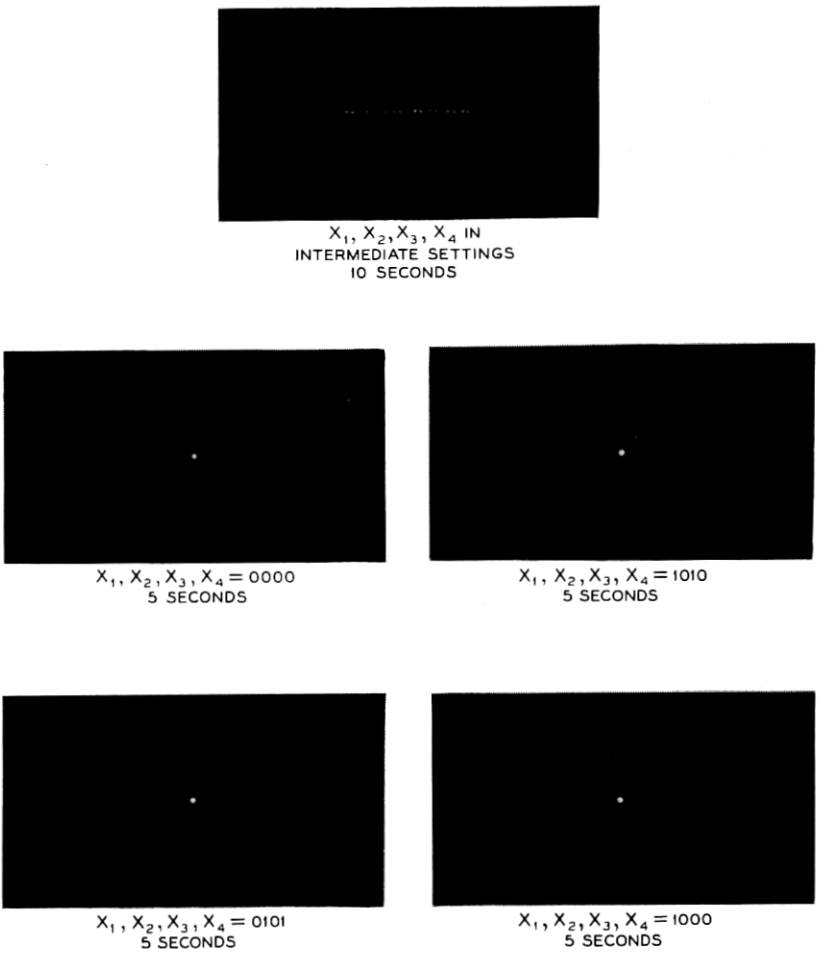

Fig. 11 — Microphotographs of spot patterns with green filter.

might represent a stored "one." If the target is opaque, the photomultiplier does not respond and a stored "zero" is inferred. A simple target could be a card with holes punched through it at some of the positions in the matrix. Since we could substitute cards with different information content, this is a semipermanent memory. In a memory application, we desire a very high storage capacity, and hence a matrix consisting of very many positions of the beam. We have shown in our section on diffraction that a high density of positions is possible; however, it then becomes difficult to position the target accurately, and this is an inherent problem

with the device. This application has the virtue that raw binary numbers serve as inputs to the storage element, and these are the type of signals most immediately available in computing machines.

6.2 *The PCM Decoder*

In the application of digital light deflection to the decoding of PCM signals, the target consists of an array of 2^n light paths, where n is the number of bits in a code group. The transparency of the light paths is quantized so that the amplitude of the output signal is different for each position. The target could be a positive photographic plate partially exposed at each of the accessible positions. The deflection banks could be conveniently used to expose the plate. The output of the photosensitive element would then be quantized PAM, and we recover the original analog signal by the usual method of passing the PAM signal through a low-pass filter. The target positioning problem is alleviated in this application because the capacity of the system is low.

6.3 *The Digital Delay Line*

Fig. 12 shows an x-deflection bank, quarter-wave plate, polarizer, delay line, analyzer, and photosensitive element arranged in line. The x-deflection bank enables us to displace the light beam in a digital manner along the x axis. Since the output light from the deflection bank is plane polarized, and the plane of polarization alternates from one position to the next, we use a quarter-wave plate and a polarizer to fix the plane of polarization that falls on the delay line. At time zero we generate

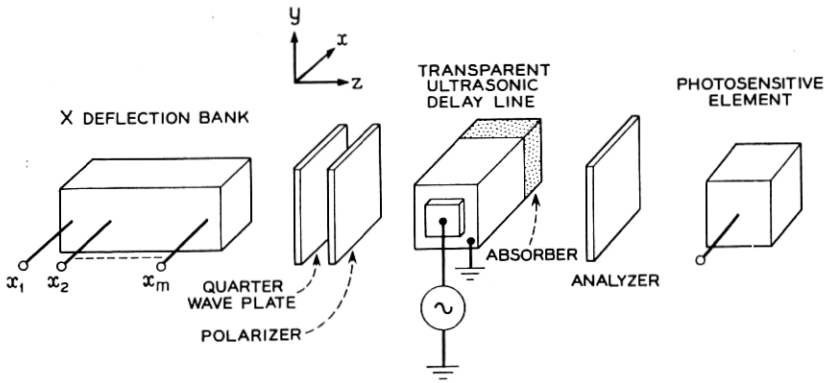

Fig. 12 — Application of digital light deflection to a digital delay line.

an ultrasonic wave in the delay line. In the absence of such a disturbance, the delay medium is transparent and isotropic, but as the disturbance passes through the position of the light beam the strain birefringence causes the light beam to be elliptically polarized. The analyzer is crossed with the polarizer and hence only transmits light to the photosensitive element when the ultrasonic wave passes through the position of the beam. Then we get an output from the photosensitive element. Thus the time at which an output results is proportional to the displacement of the beam, which in turn is determined by the state of the input variables. Thus digital light deflection can be used to make an electrically variable digital delay line. We should note that for a maximum delay line length of one inch the range of the device would be approximately 10 μsec, since sound travels in solids at roughly 0.1 in. per μsec. The time resolution would depend on the bandwidth of the delay line and the shape of the amplitude over the cross section of the light beam.

VII. CONCLUSIONS

A simple method of deflecting a light beam in a digital manner has been demonstrated. The method has the virtue of requiring only n two-level inputs for a set of 2^n possible outputs, and thus the inputs to the deflecting mechanisms are binary signals. Deflection rates above about 1 mc and with reasonable power requirements will depend on the development of optical modulator materials substantially more efficient than KDP.

VIII. ACKNOWLEDGMENTS

It is a pleasure to acknowledge the many helpful suggestions of and discussions with Messrs. J. E. Geusic, T. R. Meeker, J. H. Rowen, H. E. D. Scovil, and J. C. Skinner. I am also pleased to acknowledge the help of Miss B. T. Dale and Miss M. C. Grey, who programmed the diffraction analysis.

APPENDIX A

Fig. 13 shows the angles and directions in the uniaxial crystal with which we shall be concerned. The faces of the crystal are normal to the z axis; the optic axis of the crystal lies in an xz plane and at an angle θ with the z axis. The incident light is assumed to be a plane wave propagating in the z direction. In general the beam will be split into the ordinary ray, which passes through the crystal in a straight line, and the extraordinary ray, which is displaced.

Fig. 14 is a diagram showing the geometrical configuration of the wave normal, $\bar{s}$, and the optic axis, c. We have chosen to solve the more general

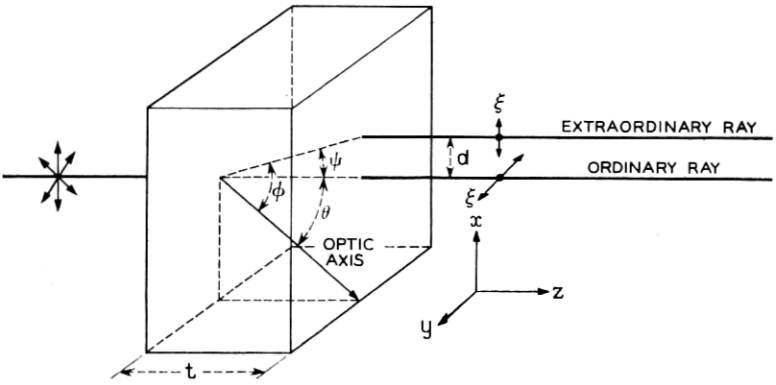

Fig. 13 — Angles and directions in uniaxial crystal.

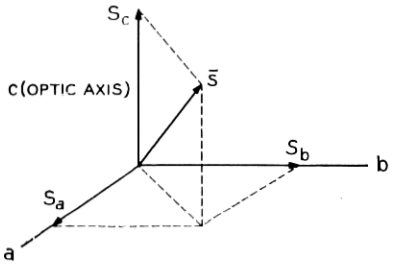

Fig. 14 — Wave normal and the crystallographic direction in the uniaxial media.

problem since the added complexity introduced is not great. In the uniaxial medium, we have[7]

$$V_a = V_b = V_0 = c/n_0 \tag{24}$$

and

$$V_c = V_e = c/n_e . \tag{25}$$

Making use of Fresnel's equation of wave normals,

$$\frac{s_a^2}{V_p - V_a^2} + \frac{s_b^2}{V_p^2 - V_b^2} + \frac{s_c^2}{V_p^2 - V_c^2} = 0, \tag{26}$$

where V_p is the normalized phase velocity, we find the two solutions

$$V_p^2 = V_0^2 \tag{27}$$

$$V_p^2 = V_0^2 \cos^2 \theta + V_e^2 \sin^2 \theta. \tag{28}$$

Born and Wolf[7] give the relations between the components of the ray vector and the components of the wave normal

$$t_k = \frac{s_k}{V_p V_r}\left(V_p^2 + \frac{g^2}{V_p^2 - V_k^2}\right) \tag{29}$$

where

$$g^2 \equiv V_p^2(V_r^2 - V_p^2) = \frac{1}{\left(\frac{s_a}{V_p^2 - V_a^2}\right)^2 + \left(\frac{s_b}{V_p^2 - V_b^2}\right)^2 + \left(\frac{s_c}{V_p^2 - V_c^2}\right)^2}. \tag{30}$$

Substituting in $V_p^2 = V_0^2$ we find that

$$g^2 = 0 \tag{31}$$

$$V_r^2 = V_p^2 = V_0^2 \tag{32}$$

$$t_k = s_k . \tag{33}$$

Thus, for the ordinary ray, the ray vector and wave normal coincide. If we substitute our second solution for the phase velocity into (29) and (30) we find

$$g^2 = (V_c^2 - V_0^2)^2 \sin^2\theta \cos^2\theta \tag{34}$$

$$V_r^2 = \frac{V_e^4 \sin^2\theta + V_0^4 \cos^2\theta}{V_e^2 \sin^2\theta + V_0^2 \cos^2\theta} \tag{35}$$

$$t_k = \frac{S_k}{V_p V_r}\left[\frac{V_e^2(V_e^2 - V_k^2)\sin^2\theta + V_0^2(V_0^2 - V_k^2)\cos^2\theta}{V_e^2 \sin^2\theta + V_0^2 \cos^2\theta - V_k^2}\right]. \tag{36}$$

This is as far as we care to carry the general case. For our more special consideration, let the b axis of Fig. 14 coincide with the y axis of Fig. 13; of course, the c axis is the optic axis, and the wave normal $\bar{s}$ points along the z axis. Thus $\bar{s}$ lies in the ac plane so that

$$s_a = \sin\theta, \qquad s_b = 0, \qquad s_c = \cos\theta. \tag{37}$$

If φ is the angle between the ray vector and the c direction, then by use of (36), we find

$$\tan\varphi = (V_e^2/V_0^2)\tan\theta = (n_0^2/n_e^2)\tan\theta. \tag{38}$$

Then the tangent of the angle between the ray vector and the z axis will be

$$\tan\psi = \tan(\varphi - \theta) = \frac{\tan\varphi - \tan\theta}{1 + \tan\varphi\tan\theta} \tag{39}$$

$$= \frac{\left(\frac{n_0^2}{n_e^2} - 1\right) \tan \theta}{1 + \frac{n_0^2}{n_e^2} \tan^2 \theta}. \tag{40}$$

Also, (35) becomes

$$V_r^2 = \frac{1}{n_r^2} = \frac{\frac{1}{n_e^4} \sin^2 \theta + \frac{1}{n_0^4} \cos^2 \theta}{\frac{1}{n_e^2} \sin^2 \theta + \frac{1}{n_0^2} \cos^2 \theta}, \tag{41}$$

hence

$$n_r^2 = \frac{1 + \frac{n_0^2}{n_e^2} \tan^2 \theta}{\frac{1}{n_0^2} + \frac{n_0^2}{n_e^4} \tan^2 \theta}, \tag{42}$$

where n_r is the refractive index for the extraordinary ray. By setting the first derivative of $\tan \psi$ with respect to $\tan \theta$ equal to zero, we may find the orientation which gives the greatest displacement of the extraordinary ray. This results in

$$\tan \theta = \frac{n_e}{n_0} \tag{43}$$

$$\tan \psi = \frac{n_0^2 - n_e^2}{2 n_e n_0} \tag{44}$$

$$n_r = \sqrt{\frac{2 n_0^2 n_e^2}{n_0^2 + n_e^2}}. \tag{45}$$

If t is the dimension of the uniaxial crystal in the z direction, then the displacement, d, of the extraordinary ray will be

$$d = \left(\frac{n_0^2 - n_e^2}{2 n_e n_0}\right) t \tag{46}$$

if the crystal has the optimum orientation.

We may note that in the negative uniaxial crystal, where $n_0 > n_e$, the extraordinary ray propagates away from the optic axis, whereas the situation is reversed in the positive crystal.

APPENDIX B

The light incident on the aperture, of radius a, is assumed to be a plane wave with wave number $k = 2\pi/\lambda$ and amplitude A. The distance S

from an element of area in the aperture to a point, P, on a sphere of radius R is expanded in a Taylor series expansion about the radial distance, ρ, from the center of the aperture (and sphere) to the element of area in the aperture.

$$S = R - \rho \sin \theta \cos \Phi \cdots . \tag{47}$$

Here θ is the angle between the radius vector to the element of area on the sphere and the cylindrical axis, Z; and Φ is the angle between the plane containing R and the cylindrical axis, and the radius vector to the element of area in the aperture. Fig. 15 shows these elements in their

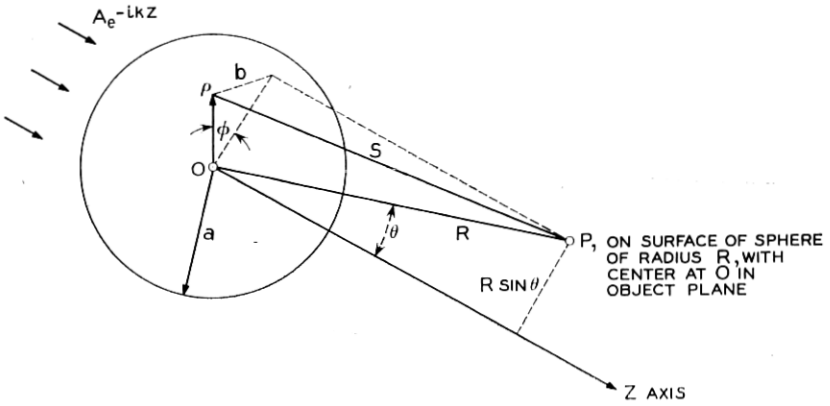

Fig. 15 — Angles and dimensions used to determine $E(\theta)$.

proper relation to one another. If the incident light has an electric field vector of the form

$$E = Ae^{-ikz} \tag{48}$$

then the electric field intensity on the sphere as a function of θ is, for small θ

$$E(\theta) = \frac{k}{2\pi} \int_0^{2\pi} \int_0^a \frac{A \exp[-ik(R - \rho \sin \theta \cos \Phi)]}{R - \rho \sin \theta \cos \Phi} \rho \, d\rho \, d\Phi. \tag{49}$$

Since $\rho \sin \theta \cos \Phi \ll R$, only the phase contribution is significant.

$$E(\theta) = \frac{kAe^{-ikR}}{2\pi R} \int_0^{2\pi} \int_0^{\rho} \rho \exp(ik\rho \sin \theta \cos \Phi) \, d\rho \, d\Phi. \tag{50}$$

Equation (50) is a standard integral with the value

$$E(\theta) = \frac{ka^2 A e^{-ikR}}{R} \left(\frac{J_1(ka \sin \theta)}{ka \sin \theta} \right). \tag{51}$$

Since the case of unity magnification is to be considered, it is assumed that the only significant function of the lens would be to cause the image and object spaces to be mirror images of each other if there were no stop at the lens. Thus, we have a section of a spherical wave to consider with a known phase and amplitude distribution. Fig. 16 shows the angles and distances under consideration. The angle θ retains its original meaning and Φ is once again a dummy variable; ρ now is the distance from the

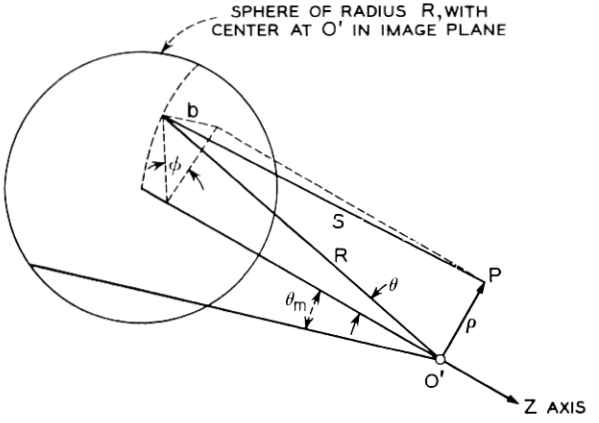

Fig. 16 — Angles and dimensions used to determine $E(\rho)$.

center of the image to the point in the image under consideration. Here S is the distance from an element of area on the sphere to the point, P, in the image plane, and is expanded about ρ.

$$S = R - \rho \sin \theta \cos \Phi + \cdots . \tag{52}$$

Hence the intensity at ρ is

$$E(\rho) = \frac{k}{2\pi} \int_0^{\theta_m} \int_0^{2\pi} \frac{E(\theta) \exp [-ik(R - \rho \sin \theta \cos \Phi)]}{R - \rho \sin \theta \cos \Phi} R \sin \theta \, d\theta \, d\Phi. \tag{53}$$

The approximation is once again made that $\rho \sin \theta \cos \Phi \ll R$:

$$E(\rho) = \frac{kRe^{-ikR}}{2\pi} \int_0^{\theta_m} \int_0^{2\pi} E(\theta) \exp (ik\rho \sin \theta \cos \Phi) \sin \theta \, d\theta \, d\Phi \tag{54}$$

and, putting in the previously determined expression for $E(\theta)$,

$$E(\rho) = (ka)^2 A e^{-i2kR} \int_0^{\theta_m} \int_0^{2\pi} \frac{J_1(ka \sin \theta)}{ka} \cdot \exp\,(ik\rho \sin \theta \cos \Phi)\, d\theta\, d\Phi \tag{55}$$

and integrating first over Φ,

$$E(\rho) = (ka) A e^{-i2kR} \int_0^{\theta_m} J_1(ka \sin \theta) J_0(k\rho \sin \theta)\, d\theta. \tag{56}$$

The integral in (56) is not available analytically; hence we resort to numerical procedures. The f number of the system and θ_m are intimately related,

$$\tan \theta_m = \frac{1}{4F} \tag{57}$$

and for small angles,

$$\theta_m \approx \frac{1}{4F}. \tag{58}$$

Since we wish to evaluate the crosstalk ratio, it is also necessary to integrate $[E(\rho)]^2$ over a circle of radius a located in the image plane. Fig. 17 defines the center-to-center separation as d and the local cylindrical coordinates ρ' and φ. We find by the usual geometrical considerations that

$$\rho = [d^2 - 2\, d\rho' \cos \varphi + \rho'^2]^{\frac{1}{2}}. \tag{59}$$

However, no approximations are in order here, as ρ' and d are of the same order of magnitude. Therefore the integral

$$P(d) = \int_0^{2\pi} \int_0^{a} \rho' E^2([d^2 - 2d\rho' \cos \varphi + \rho'^2]^{\frac{1}{2}})\, d\rho'\, d\varphi \tag{60}$$

results in the power falling on the circle of radius a and being displaced from the center of the image by distance d. The crosstalk ratio, C, will

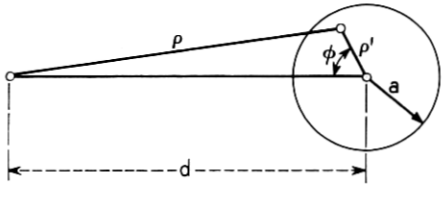

Fig. 17 — Circle of integration for determining crosstalk ratio and loss.

be defined as

$$C = 10 \log_{10} \left(\frac{P(0)}{P(d)} \right) \text{db}. \tag{61}$$

Also, we are in a position to evaluate the loss through the system

$$L = 10 \log_{10} \left(\frac{\pi a^2 A^2}{P(0)} \right) \text{db}, \tag{62}$$

that is, the db ratio of the power admitted to the system by the aperture to the power falling on a circle of radius a centered on the image. The amount of light lost from that emitted by the source depends strongly on the type of source and focusing at the aperture. If the source is focused on the lens system in the absence of the aperture, then our equations are still good approximations, although such illumination would not be plane.

REFERENCES

1. Caldwell, S. H., *Switching Circuits and Logical Design*, Wiley, New York, 1959, Chap. 7.
2. Sears, F. W., *Optics*, Addison-Wesley, Boston, 1949, p. 181.
3. Dillon, J. F., Jr., Optical Properties of Several Ferrimagnetic Garnets, J. Appl. Phys., **29**, Mar., 1958, p. 539.
4. *American Institute of Physics Handbook*, ed. Gray, D. E., McGraw-Hill, New York, 1957, pp. 6-94 to 6-97.
5. Zwicker, B. and Scherrer, P., Electro-Optical Properties of the Rochelle Salt Electrical Crystals, KH_2PO_4 and KD_2PO_4 , Helvetica Physica Acta, **17**, 1944, pp. 346–373.
6. Kaminow, I. P., and Harding, G. O., Complex Dielectric Constant of KH_2PO_4 at 9.2 Gc/sec, Phys. Rev., **129**, Feb., 1963, pp. 1562–66.
7. Born, M. and Wolf, E., *Principles of Optics*, Pergamon Press, New York, 1959, Chap. 14.